SUPPLEMENTARY MATERIALS

THERMODYNAMICS AND KINETICS OF PHASE TRANSFORMATION IN TWO-COMPONENT SUBMONOLAYER FILMS

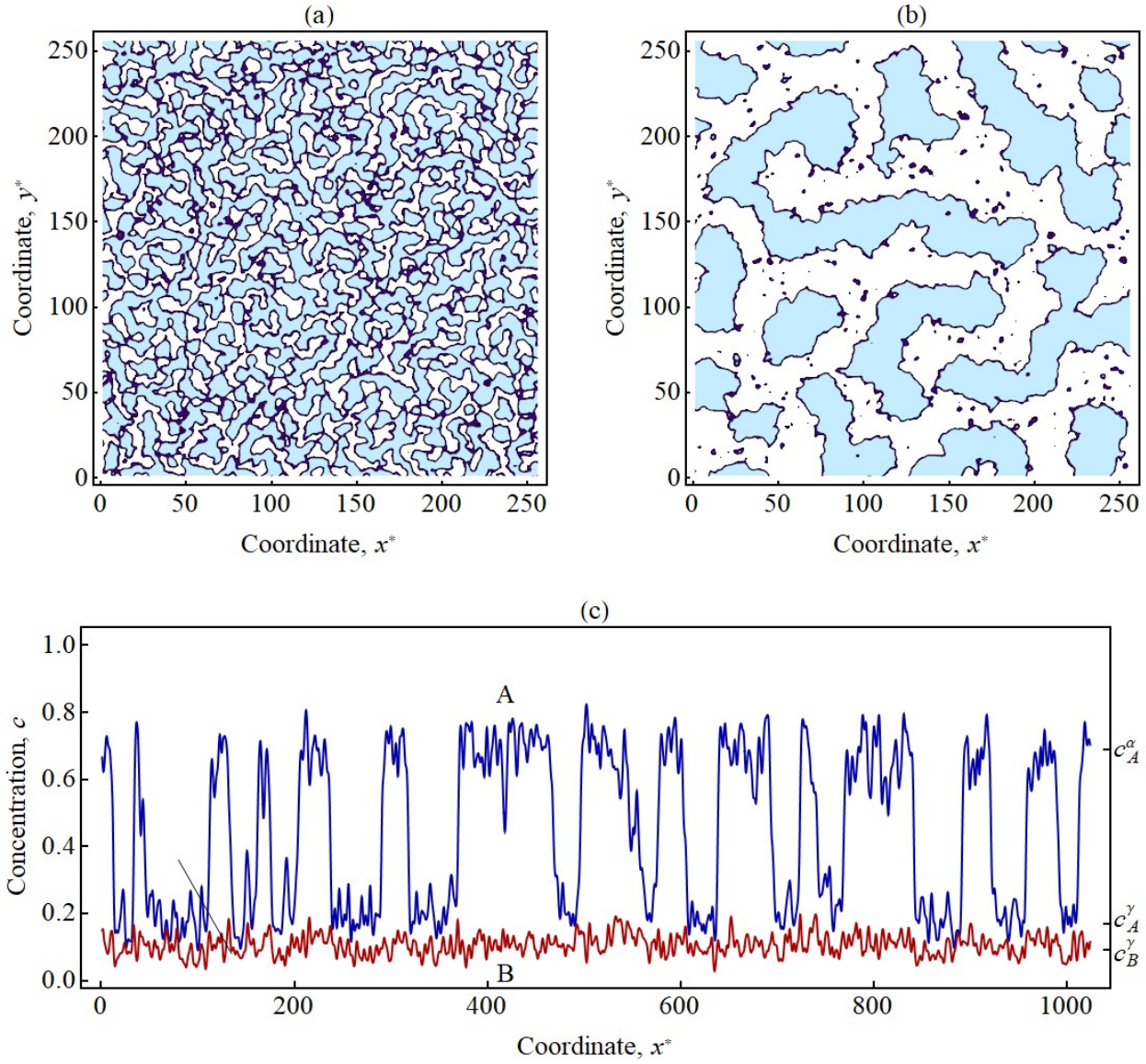

Figure S1. Simulation results of the phase transformation in submonolayer film with initial concentrations $c_A = 0.4$ and $c_B = 0.1$ at the temperature $T^* = 0.9$. Cyan islands in Figs. a and b show the A-rich regions at the substrate ($c_A > 0.4$) at the time points $t^* = 125$ and $t^* = 33875$, respectively. Figure c shows the concentration profiles across the section with coordinate $y^* = 300$ for atoms A (blue line) and B (red line). Right axis shows the values of equilibrium concentrations from table 1.

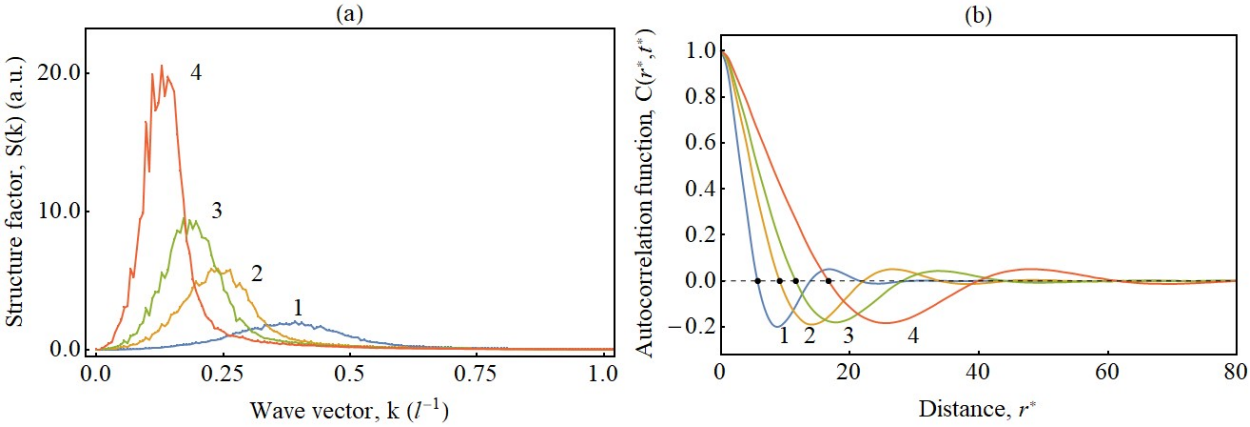

Figure S2. Calculation of structure factor (figure a) and autocorrelation function (figure b) for spinodal decomposition of submonolayer film with initial concentrations $c_A = 0.4$ and $c_B = 0.1$ at the temperature $T^* = 0.9$. Lines are calculated by equations (12) for different time points: $t^* = 375$, $t^* = 2625$, $t^* = 6375$, $t^* = 25125$. Black points (figure b) show the coordinate of first zero of autocorrelation function.

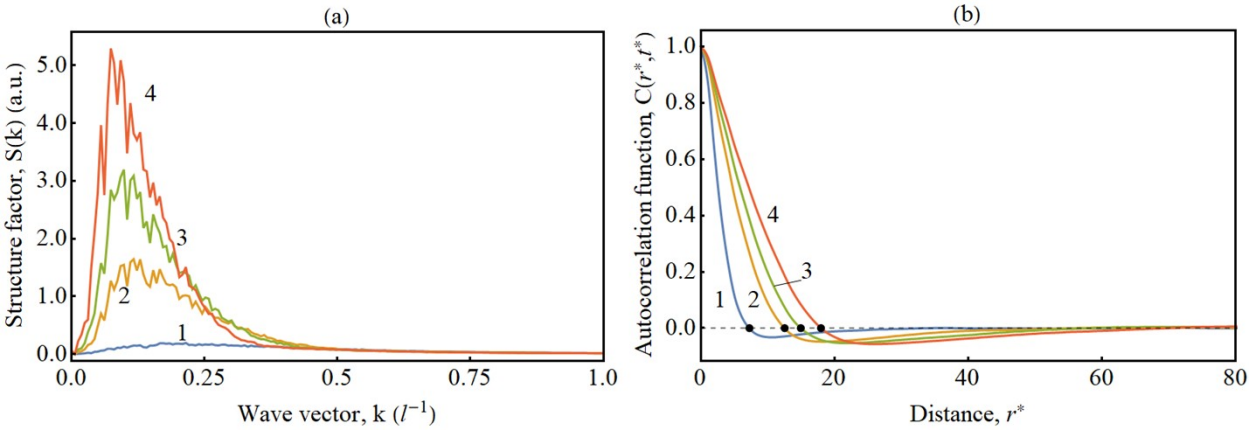

Figure S3. Calculation of structure factor (figure a) and autocorrelation function (figure b) for nucleation and growth of islands in submonolayer film with initial concentrations $c_A = 0.2$ and $c_B = 0.05$ at the temperature $T^* = 0.9$. Lines are calculated by equations (13) for different time points: $t^* = 1375$, $t^* = 6375$, $t^* = 12652$, $t^* = 35625$. Black points (figure b) show the coordinate of first zero of autocorrelation function.

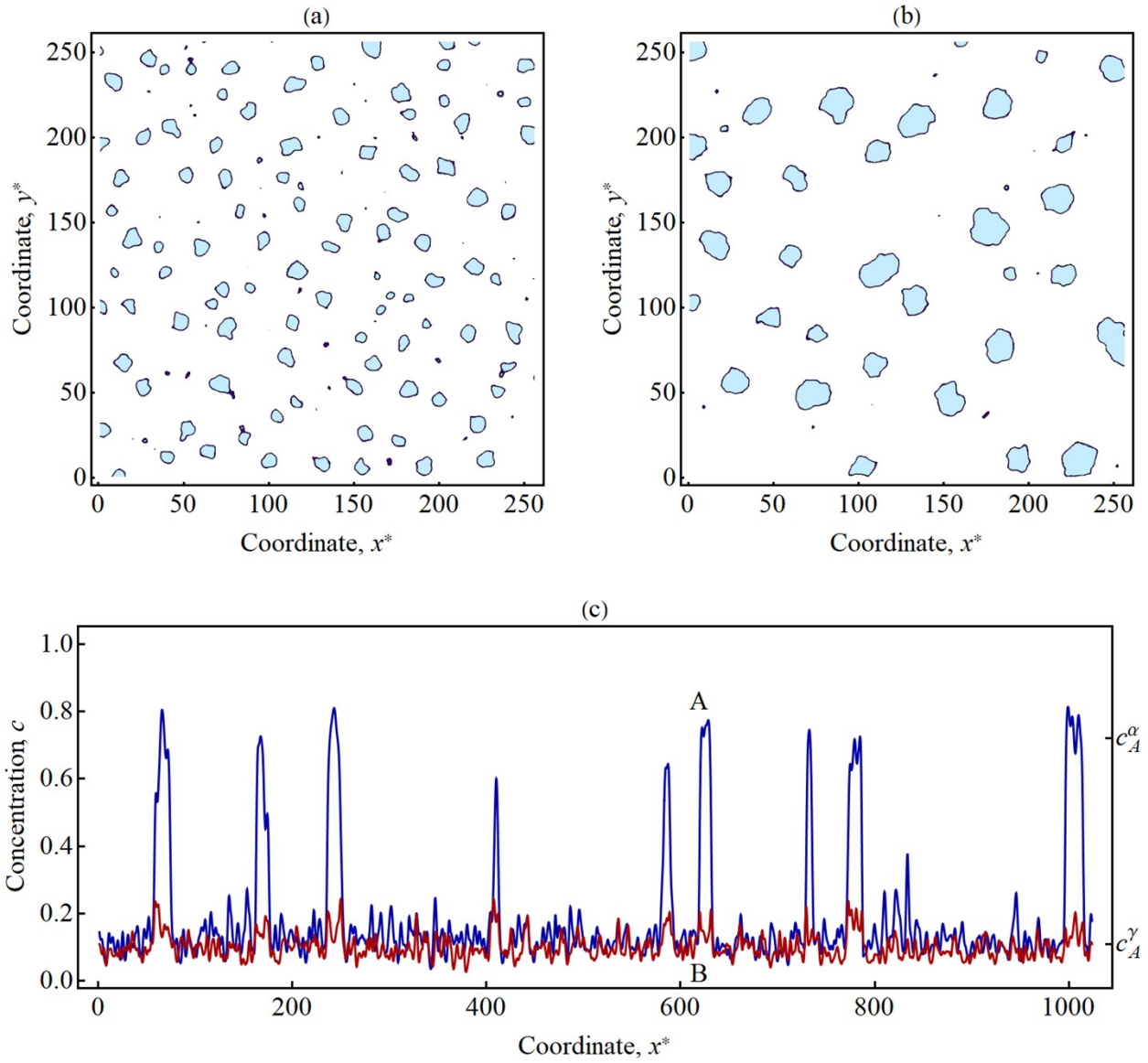

Figure S4. Simulation results of the phase transformation in submonolayer film with initial concentrations $c_A = 0.17$ and $c_B = 0.1$ at the temperature $T^* = 0.8$. Cyan islands in figures (a) and (b) show the A-rich regions at the substrate ($c_A > 0.4$) at the time points $t^* = 750$ and $t^* = 22875$, respectively. Figure c shows the concentration profiles across the section with coordinate $y^* = 320$ for atoms A (blue line) and B (red line). Right axis (figure c) shows the values of equilibrium concentrations from table 1

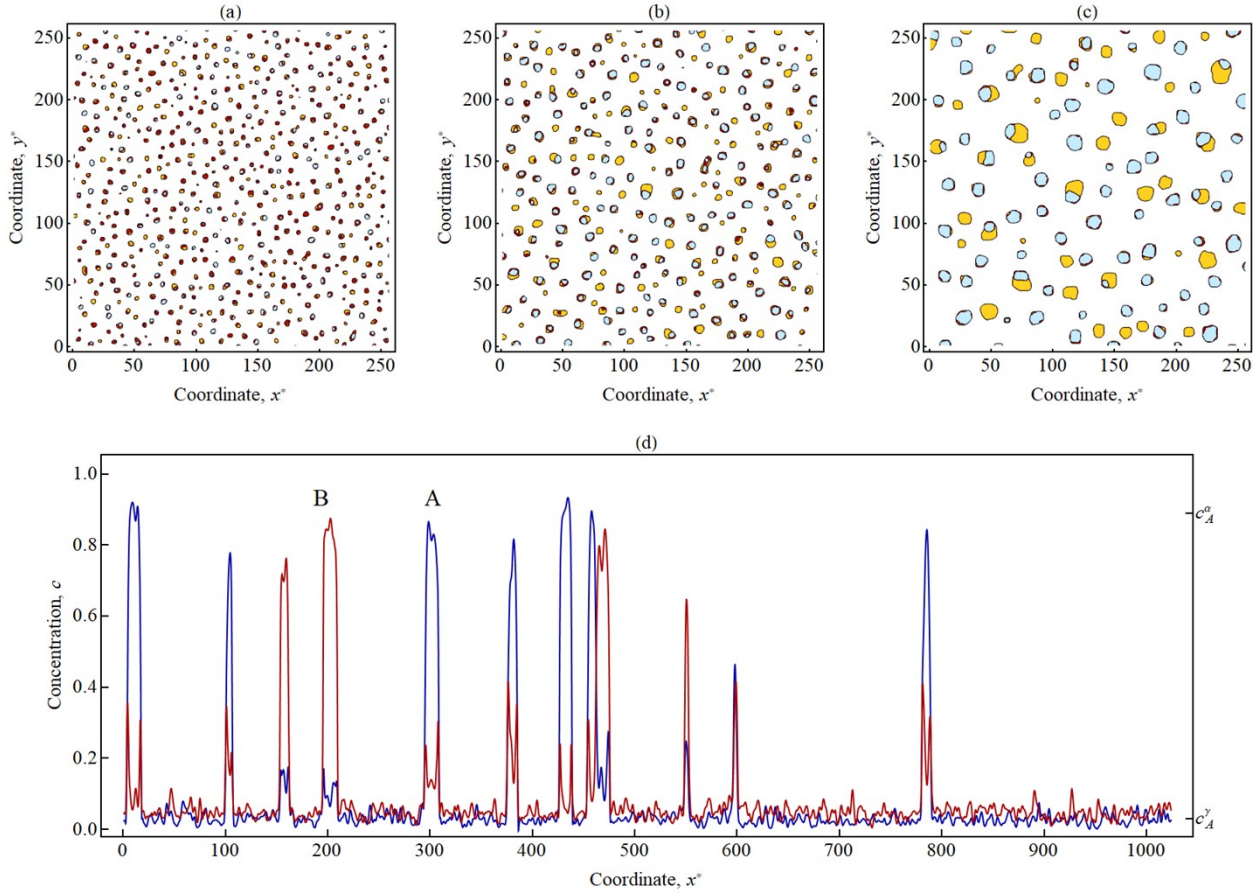

Figure S5. Simulation results of the phase transformation in submonolayer film with initial concentrations $c_A = 0.1$ and $c_B = 0.1$ at the temperature $T^* = 0.58$. Cyan, yellow, and white islands in figures (a-c) show the A-, B- and V-rich regions on the substrate ($c_A > 0.4, c_B > 0.4$) at the time points $t^* = 125$, $t^* = 1375$, and $t^* = 37500$, respectively. Figure (d) shows the concentration profiles across the section with coordinate $y^* = 320$ for atoms A (blue line) and B (red line). Right axis (figure d) shows the values of equilibrium concentrations from table 1.

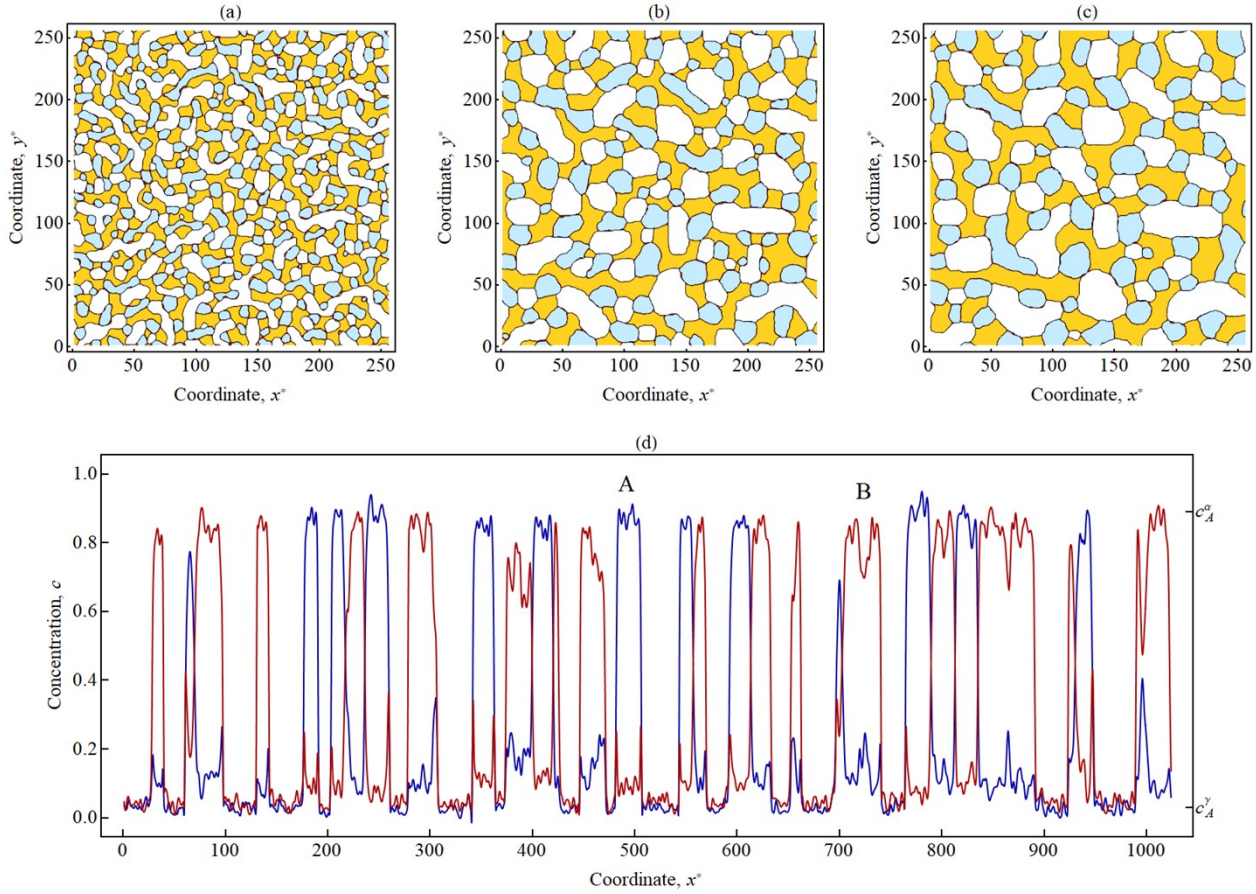

Figure S6. Simulation results of the phase transformation in submonolayer film with initial concentrations $c_A = 0.3$ and $c_B = 0.3$ at the temperature $T^* = 0.58$. Cyan, yellow, and white areas in figures (a-c) show the A-, B- and V-rich regions on the substrate ($c_A > 0.4, c_B > 0.4$) at the time points $t^* = 1375$, $t^* = 12625$, and $t^* = 37500$, respectively. Figure (d) shows the concentration profiles across the section with coordinate $y^* = 320$ for atoms A (blue line) and B (red line). Right axis (figure d) shows the values of equilibrium concentrations from table 1.

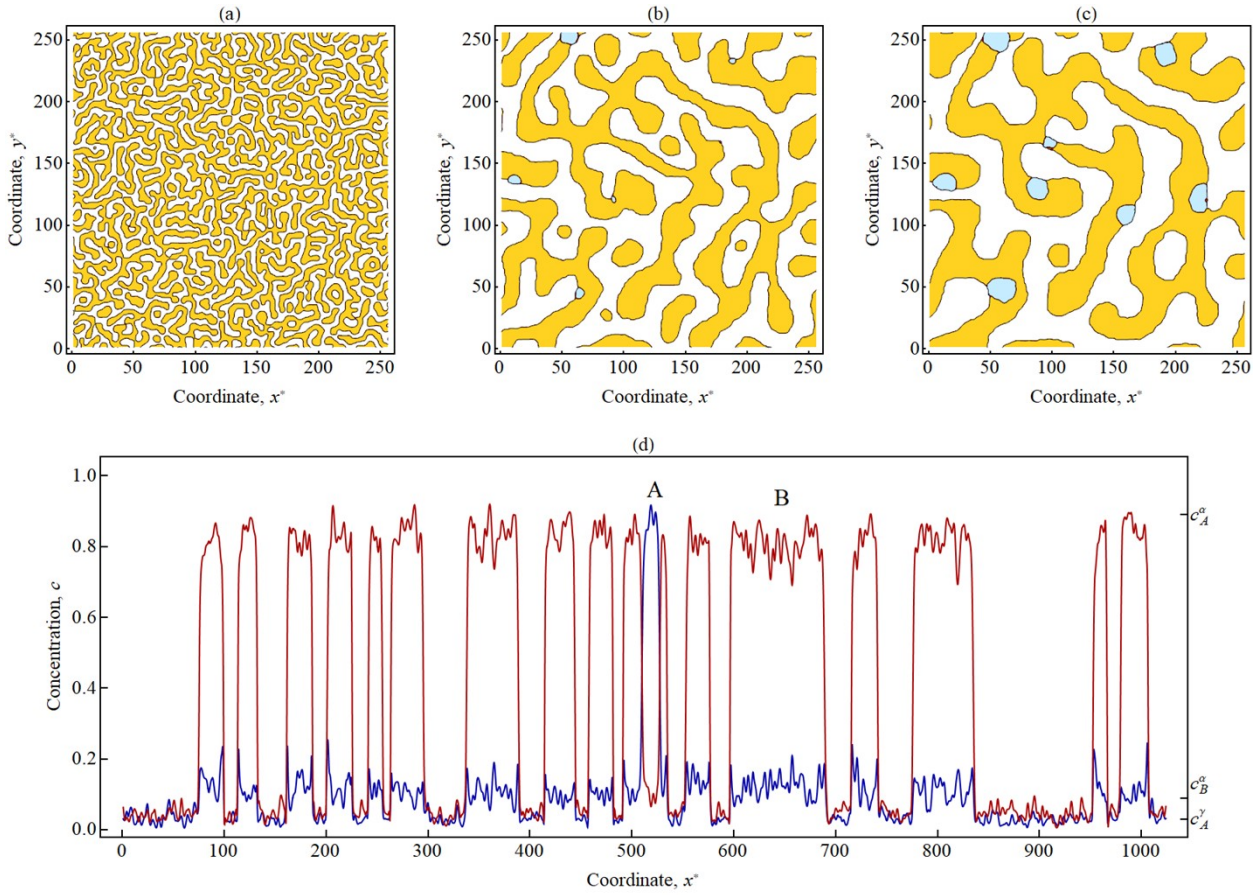

Figure S7. Simulation results of the phase transformation in submonolayer film with initial concentrations $c_A = 0.1$ and $c_B = 0.4$ at the temperature $T^* = 0.58$. Cyan, yellow, and white areas in Figs. (a-c) show the A-, B- and V-rich , respectively ($c_A > 0.4, c_B > 0.4$). Figures a-c correspond to different time points: (a) - $t^* = 1375$, (b) - $t^* = 12625$, and (c) - $t^* = 30500$. Figure (d) shows the concentration profiles across the section with coordinate $y^* = 320$ for atoms A (blue line) and B (red line) at $t^* = 30500$. Right axis (figure d) shows the values of equilibrium concentrations from table 1.

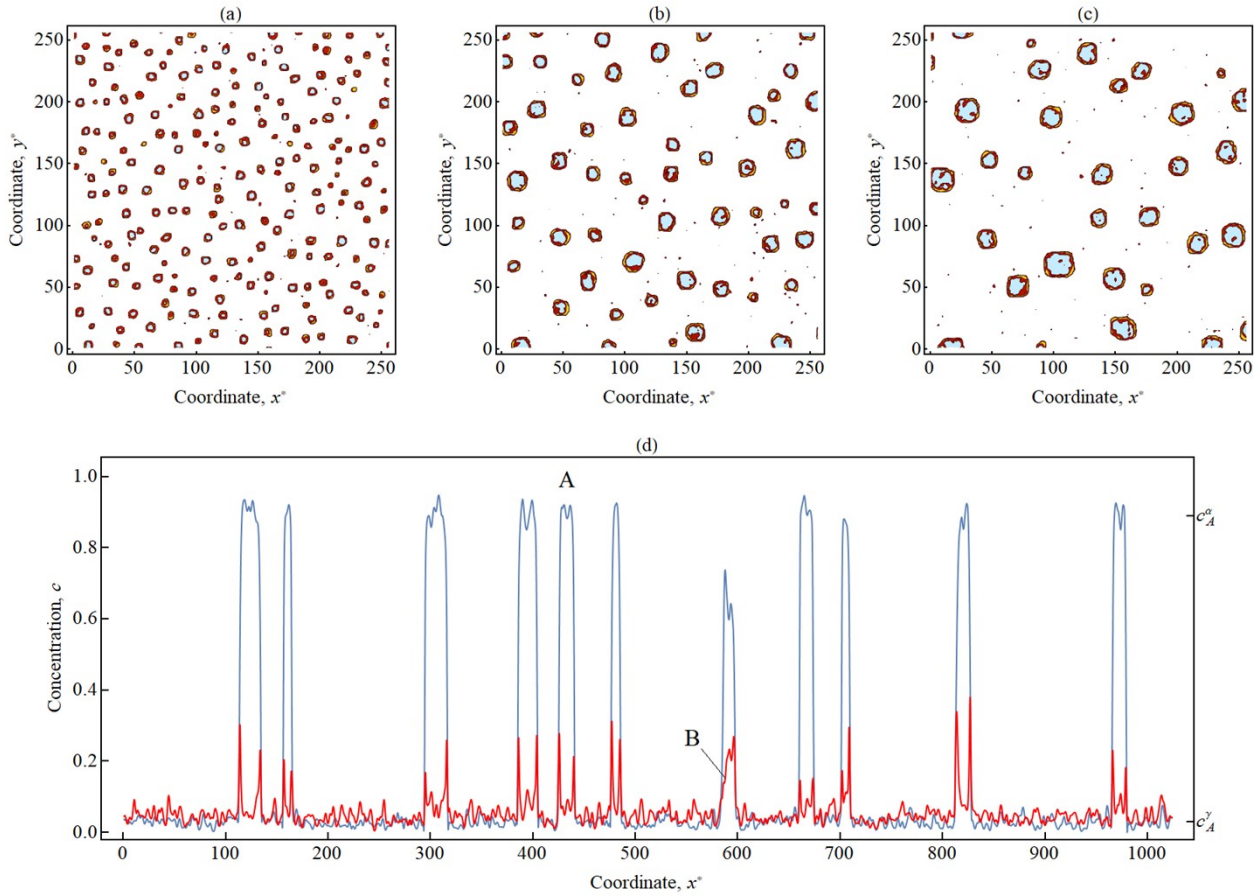

Figure S8. Simulation results of the phase transformation in submonolayer film with initial concentrations $c_A = 0.1$ and $c_B = 0.05$ at the temperature $T^* = 0.58$. Cyan, yellow, and white areas in Figs. (a-c) show the A-, B- and V-rich , respectively ($c_A > 0.4, c_B > 0.4$). Figures (a-c) correspond to different time points: (a) - $t^* = 1375$, (b) - $t^* = 3875$, and (c) - $t^* = 87500$. Figure (d) shows the concentration profiles across the section with coordinate $y^* = 320$ for atoms A (blue line) and B (red line) at $t^* = 87500$. Right axis (figure d) shows the values of equilibrium concentrations from Table 1.

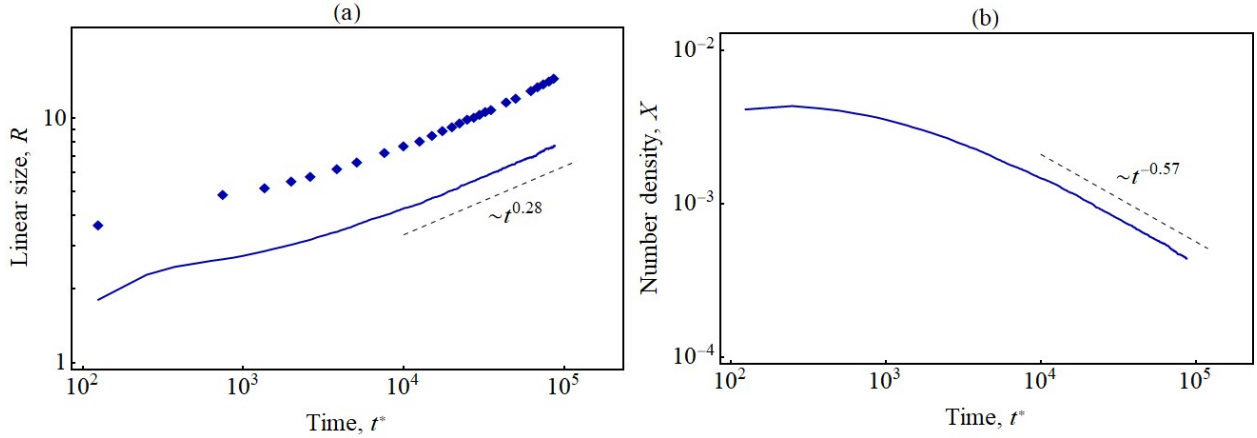

Figure S9. Dynamics of the linear size (figure a) and number density (figure b) of islands during phase transformation in two-component film with interaction parameters from Set 1 (table 1) at the temperature of $T^* = 0.58$ and initial concentration $c_A = 0.1$ and $c_B = 0.05$. Blue lines (1) and points (diamonds) correspond to A-rich phase (see figure S8). Points are calculated as first zero of autocorrelation function, and solid lines are calculated by the NN method. Dashed lines are the power-law dependences determined at the later stage of phase transformation.

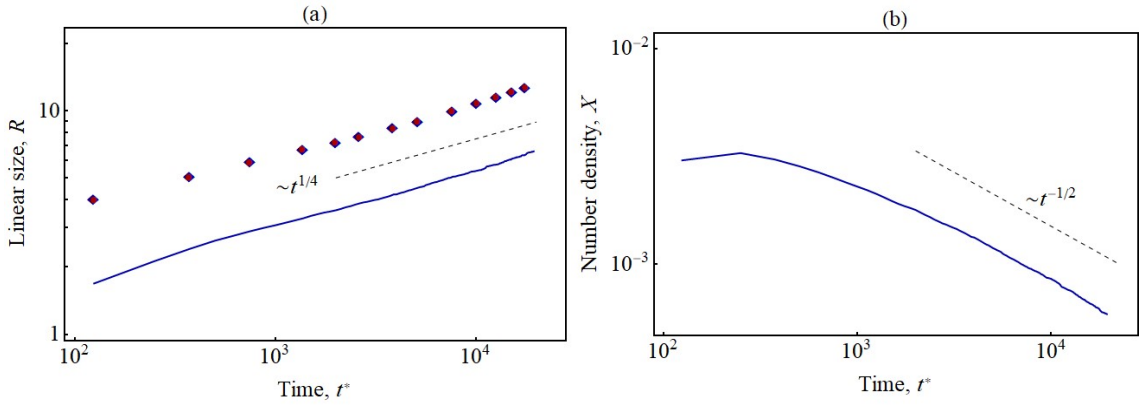

Figure S10. Dynamics of the linear size (figure a) and number density (figure b) of islands during phase transformation in two-component film with interaction parameters from Set 2 (table 1) at the temperature of $T^* = 0.9$ and initial concentration $c_A = 0.12$ and $c_B = 0.08$. Blue lines and points (diamonds) correspond to A-rich phase. Red points (circles) correspond to B-rich phase. Points are calculated as first zero of autocorrelation function, and solid lines are calculated by the NN method. Dashed lines are the power-law dependences determined at the later stage of phase transformation.

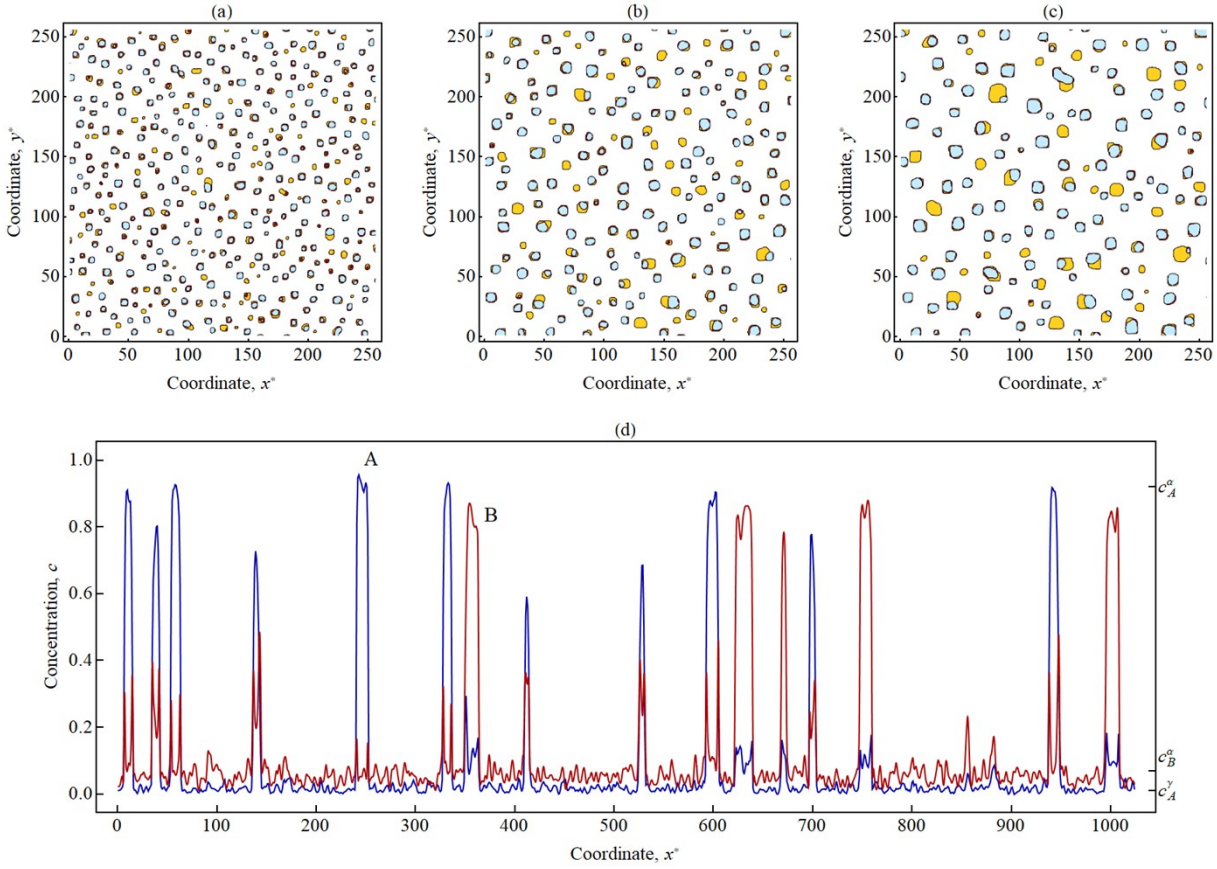

Figure S11. Simulation results of the phase transformation in submonolayer film with initial concentrations $c_A = 0.1$ and $c_B = 0.1$ at the temperature $T^* = 0.6$ for interaction parameters from Set 3 (table 1). In Figs. (a-c), cyan, yellow, and white areas show the A-, B- and V-rich regions, respectively. Figures (a-c) are drawn at different time points: (a) - $t^* = 1375$, (b) - $t^* = 6375$, and (c) - $t^* = 34000$, respectively. Figure (d) shows the concentration profiles across the section with coordinate $y^* = 320$ for atoms A (blue line) and B (red line) at $t^* = 34000$. Right axis (figure d) shows the values of equilibrium concentrations from table 1.

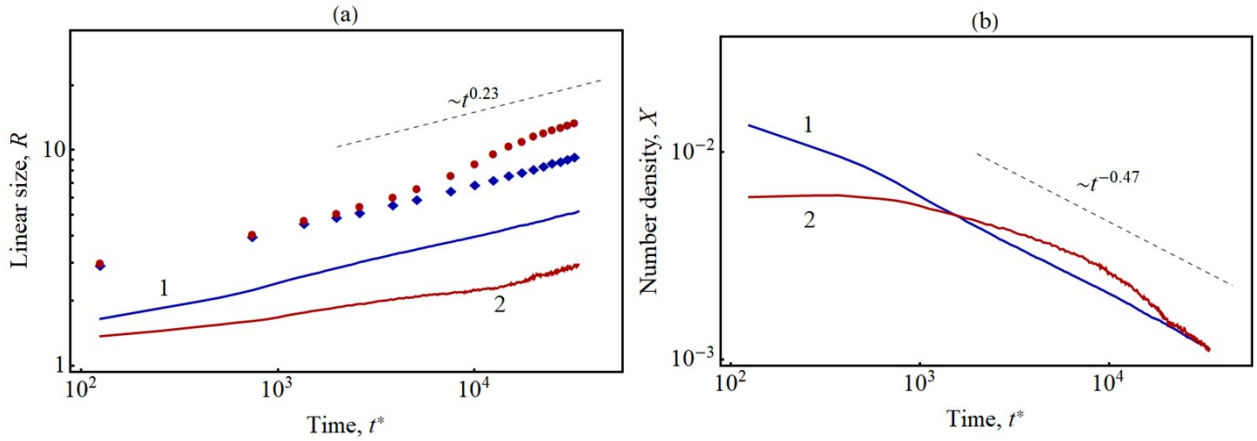

Figure S12. Dynamics of the linear size (figure a) and number density (figure b) of islands during phase transformation in two-component film with interaction parameters from Set 3 (Table 1) at the temperature of $T^* = 0.6$ and initial concentration $c_A = 0.1$ and $c_B = 0.1$. Blue lines (1) and points (diamonds) correspond to A-rich phase. Red points (circles) lines (2) correspond to B-rich phase. Points are calculated as first zero of autocorrelation function, and solid lines are calculated by the NN method. Dashed lines are the power-law dependences determined at the later stage of phase transformation for A-rich phase.

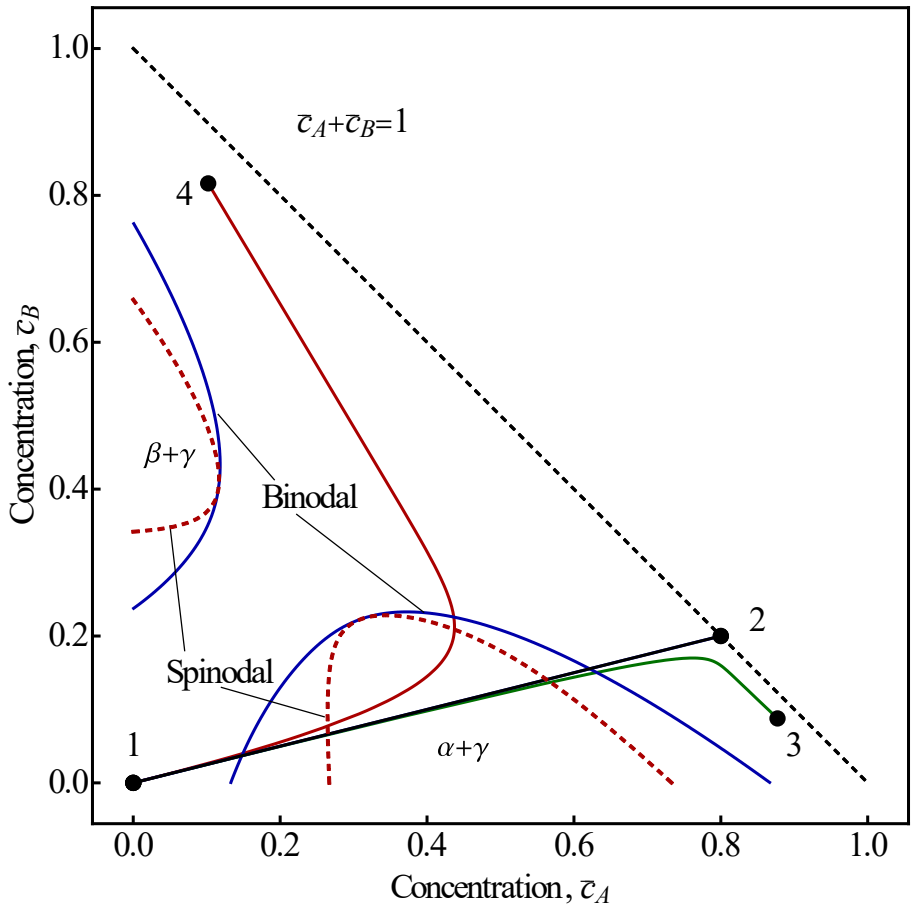

Figure S13. Phase diagram of two-component film with interaction parameters Set 1 (table 1) at the temperature of $T^* = 0.9$ with lines (1-2, 1-3, 1-4) determining change of the composition during deposition and evaporation process (figure 17).

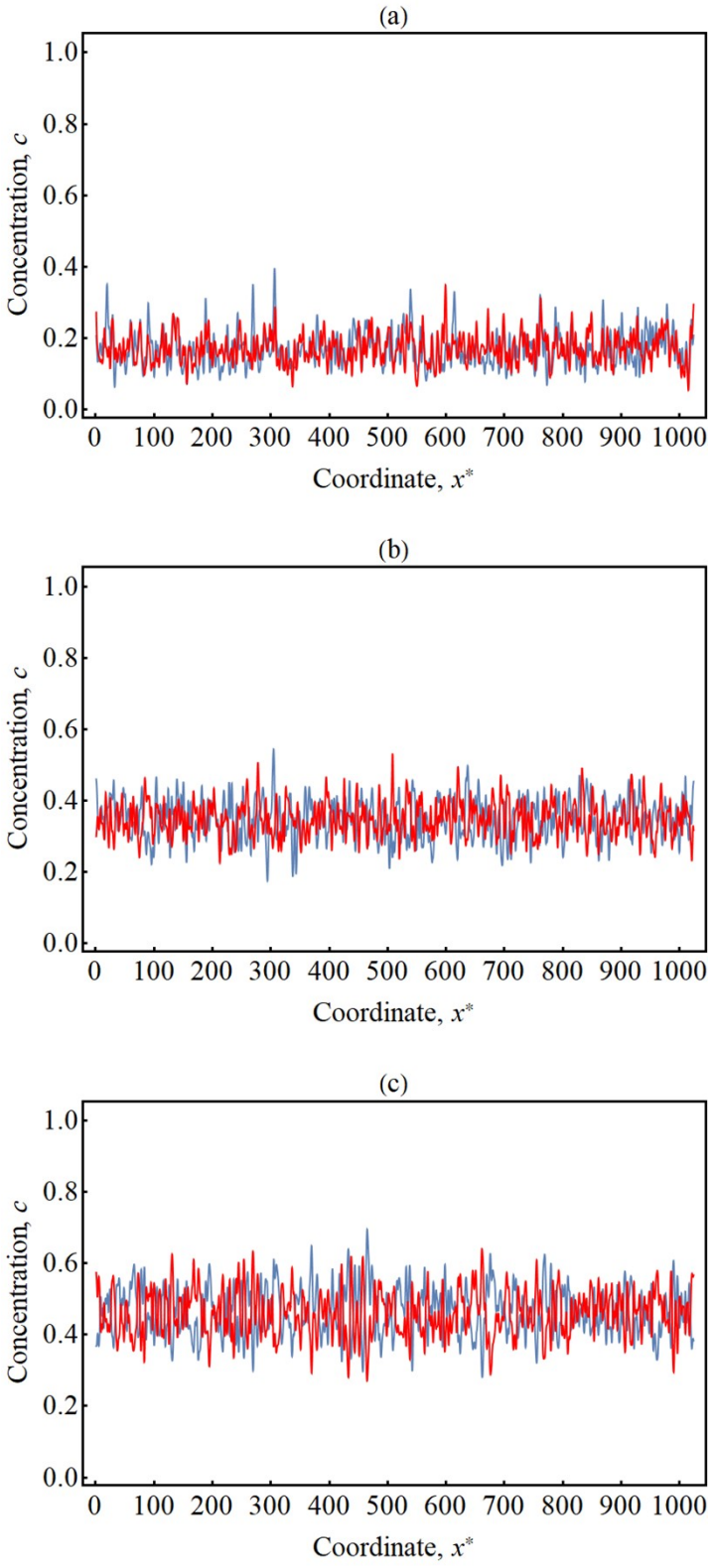

Figure S14. Dynamics of concentration profile c_A and c_B for the film with interaction parameters from Set 1 (table 1) at the temperature $T^* = 0.9$ and deposition rates $I_A^+ = 10^{-4}, I_A^- = 0, I_B^+ = 10^{-4}, I_B^- = 0$. The trajectory in $\bar{c}_A - \bar{c}_B$ space does not go through the miscibility gap (see figure 13S), so formation of new phase cannot be observed. Figures correspond to different time points: (a) - $t^* = 2000\,(\bar{c}_A = 0.17, \bar{c}_B = 0.17)$, (b) - $t^* = 5750$ $(\bar{c}_A = 0.34, \bar{c}_B = 0.34)$, (c) $t^* = 13000$ $(\bar{c}_A = 0.46, \bar{c}_B = 0.46)$

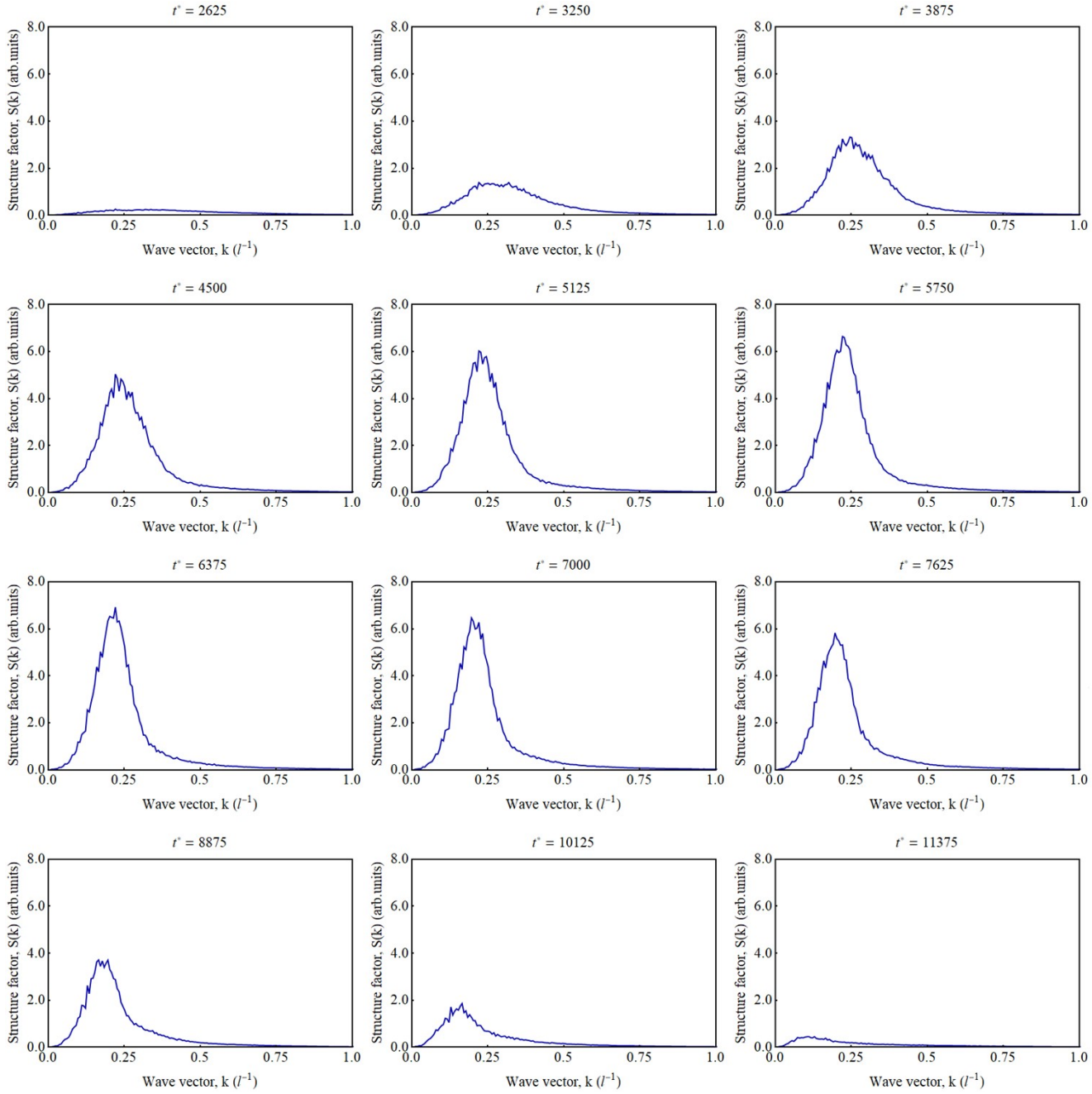

Figure S15. Dynamics of the structure factor in two-component film under PVD conditions. Deposition and evaporation rates are $I_A^{*+} = 10^{-4}, I_A^{*-} = 0, I_B^{*+} = 0.25 \cdot 10^{-4}, I_B^{*-} = 0$. Corresponding time points are given in the plot labels. Interaction parameters correspond to Set 1 from Table 1, and the temperature is $T^* = 0.9$.

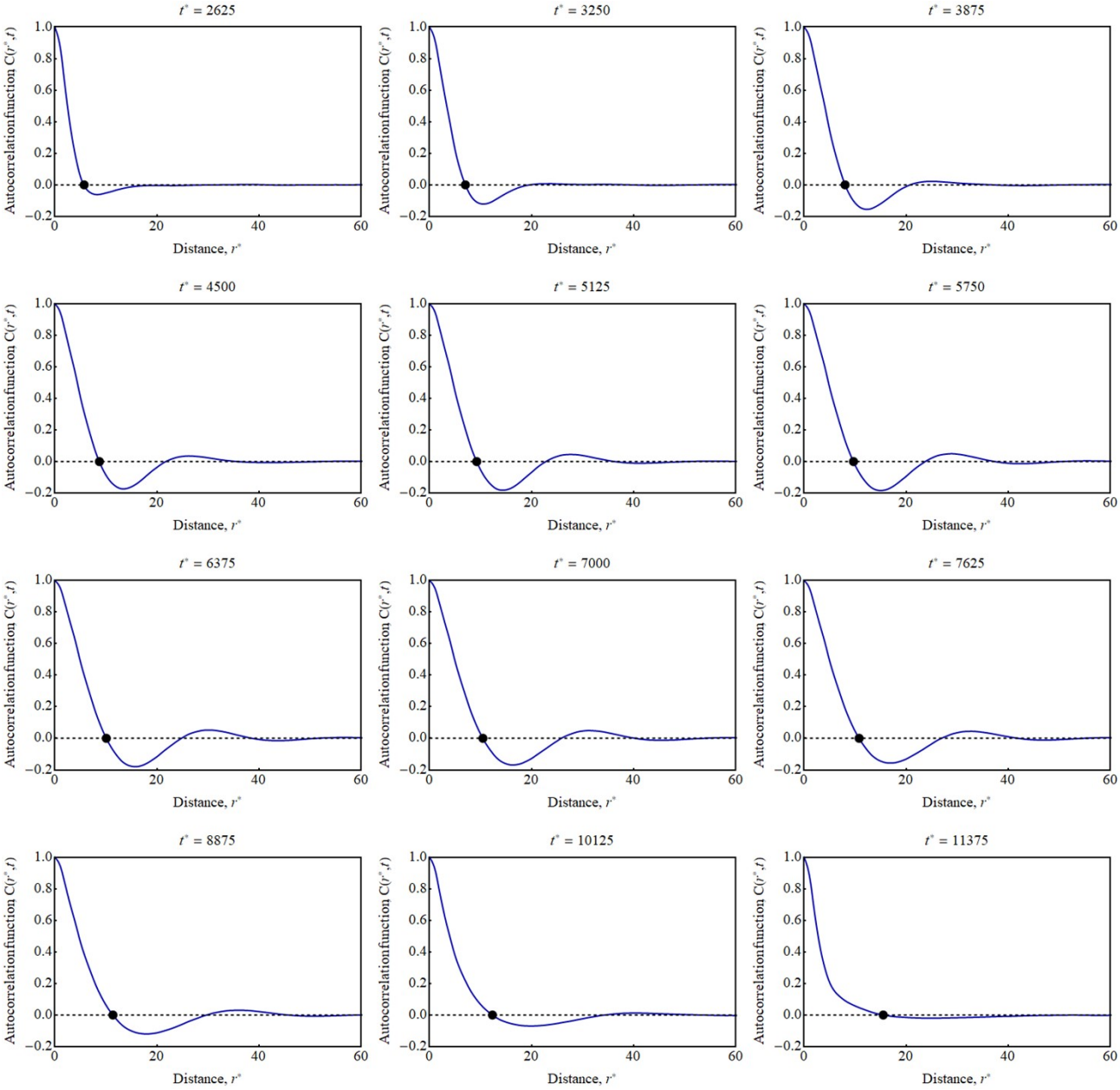

Figure S16. Dynamics of the autocorrelation function in two-component film under PVD conditions. Deposition and evaporation rates are $I_A^{*+} = 10^{-4}, I_A^{*-} = 0, I_B^{*+} = 0.25 \cdot 10^{-4}, I_B^{*-} = 0$. Corresponding time points are given in the plot labels. Interaction parameters correspond to Set 1 from table 1, and the temperature is $T^* = 0.9$. Points show the position of the first minimum of autocorrelation function.

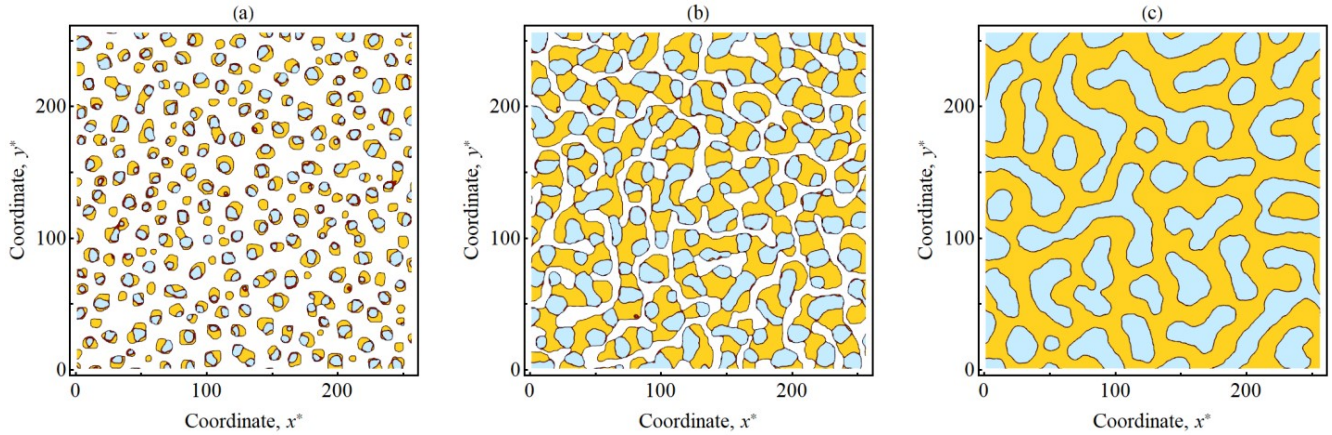

Figure S17. Dynamics of the concentration fields c_A and c_B under PVD condition with deposition and evaporation rate coefficients equal $I_A^{*+}=10^{-4}, I_A^{*-}=0, I_B^{*+}=10^{-4}, I_B^{*-}=0$. Cyan and yellow regions correspond to concentrations greater than $c_A>0.4$ and $c_B>0.4$, respectively. Figures are the snapshots at different time points t^*: (a) – 2000, (b) – 6375, (c) – 16750. Interaction parameters correspond to Set 1 from Table 1, and the temperature is $T^*=0.58$.

Movie S1. Dynamics of the concentration field c_A (left figure) under PVD condition with deposition and evaporation rate coefficients equal $I_A^{*+}=10^{-4}, I_A^{*-}=0, I_B^{*+}=0.25\cdot10^{-4}, I_B^{*-}=0$. Cyan regions correspond to concentrations greater than $c_A>0.4$. Interaction parameters correspond to Set 1 from table 1, and the temperature is $T^*=0.9$. Right figure shows the trajectory in $\bar{c}_A-\bar{c}_B$ space conjugated with the binodal and spinodal line. Running point shows the current position of the system on this trajectory.

Movie S2. Dynamics of the concentration fields c_A and c_B under PVD condition with deposition and evaporation rate coefficients equal $I_A^{*+}=10^{-4}, I_A^{*-}=0, I_B^{*+}=10^{-4}, I_B^{*-}=0$ (left figure). Interaction parameters correspond to Set 1 from table 1, and the temperature is $T^*=0.58$.

Movie S3. Dynamics of the concentration fields c_A and c_B under PVD condition with deposition and evaporation rate coefficients equal $I_A^{*+}=10^{-3}, I_A^{*-}=8.0\cdot10^{-4}, I_B^{*+}=2.5\cdot10^{-4}, I_B^{*-}=2.5\cdot10^{-5}$. Cyan and yellow regions correspond to concentrations greater than $c_A>0.4$ and $c_B>0.4$, respectively. Interaction parameters correspond to Set 1 from table 1, and the temperature is $T^*=0.58$. Right figure shows the dynamics of overall concentration deposited on the substrate. Running points correspond to current overall concentration of atoms.